DIRECT NUMERICAL SIMULATION OF SPATIALLY DEVELOPING CHANNEL MAGNETO-CONVECTION

Alex Old
School of Mechanical, Aerospace and Civil Engineering
University of Sheffield
Sheffield, S1 3JD, United Kingdom
asold1@sheffield.ac.uk

Wei Wang
Scientific Computing
Science and Technology Facilities Council
Daresbury Laboratory, WA4 4AD, United Kingdom
wei.wang@stfc.ac.uk

Shuisheng He
School of Mechanical, Aerospace and Civil Engineering
University of Sheffield
Sheffield, S1 3JD, United Kingdom
s.he@sheffield.ac.uk

ABSTRACT

Magneto-convection is the movement of an electrically conducting fluid within a magnetic field in which thermally-induced convection is significant. The combination of strong electromagnetic and buoyancy body forces result in a unique form of turbulence that differs significantly from classical hydrodynamic turbulence, with anisotropy and reduced inertial effects playing key roles. Here we consider spatially developing buoyancy-aided turbulence in a channel with single to multi-dimensional magnetic fields. This configuration is relevant to prototype liquid metal breeding blankets of fusion machines.

INTRODUCTION

Magneto-convection is encountered in several advanced industrial processes, such as semiconductor and metal manufacturing but are particularly relevant to the breeding blankets of fusion machines, in which liquid metals are circulated to produce tritium fuel and extract heat. Tokamak-based fusion reactors have a strong toroidal magnetic field and a weaker poloidal magnetic field, 5% to 10% of the toroidal component for typical tokamaks but as high as 40% for spherical tokamaks. This study will consider a fundamental orientation: a vertical channel, strongly heated on one side, in a buoyancy-aided configuration. Boussinesq equations of strong buoyancy influenced flows in an infinite domain have an analytical solution of so-called elevator-modes: pairs of ascending and descending vertical jets. Such jets typically break down to turbulence due to secondary instabilities in hydrodynamic flows but can be partially stabilised in magnetohydrodynamic flows by a strong transverse magnetic field. Previous work has predominantly studied buoyancy-opposed flow in which jets appear in a quasi-periodic evolution which breaks down into large quasi-two-dimensional vortices, resulting in high-amplitude, low frequency fluctuations of temperature (magneto-convective fluctuations, MCFs) (Zhang & Zikanov (2018)). Buoyancy-aided magneto-convection has recieved far less attention despite it's role as the flow regime behind the plasma-facing first wall. Vetcha *et al.* (2013) undertook a two dimensional numerical analysis of steady-state buoyancy aided flow in a duct and identified various regimes of two dimensional turbulence, with a similar inflectional instability mechanism to buoyancy-opposed flows but to a far less violent extent given stable temperature stratification. Additionally, a Kelvin-Helmholtz type secondary boundary layer instability was identified. A stability parameter of buoyancy-influenced flows can be described by three dimensionless parameters of Reynolds number ($Re = UL/\nu$), Hartmann number ($Ha = BL\sqrt{\sigma/\mu}$) and Grashof number ($Gr = g\beta\Delta T d^3/\nu^2$), given in Equation 1. Stability criterion $\Pi_{crit} \approx 16$ for a transverse magnetic field in a buoyancy-opposed orientation (Zikanov *et al.* (2021)).

$$\Pi = \frac{Gr}{Re \cdot Ha} \tag{1}$$

A transverse magnetic field component is known to be the most effective at suppressing turbulent fluctuations due to modification of the mean velocity profile through the induced flow-opposing Lorentz force (Lee & Choi (2001)). A streamwise magnetic field interacts with turbulent fluctuations, suppressing velocity variations in the streamwise direction through a conversion to electrical energy via the Lorentz force and then to heat from subsequent ohmic dissipation (A. Alemany *et al.* (1979)). Previous numerical study of magneto-convective flows have used the quasi-two-dimensional approximation (Sommeria & Moreau (1982)) to simplify governing equations solved in the assumption that in the limit of a strong 1D magnetic field, velocity fluctuations are completely suppressed along magnetic field lines. In a multi-dimensional magnetic field, this methodology is not valid.

This study therefore intends to investigate the following questions: (i) How do wall-normal, streamwise and inclined magnetic fields compare in suppression of primarily buoyancy produced turbulence? (ii) How might observed mechanisms extrapolate to higher magnitude parameters of a fusion breeding blanket?

METHODOLOGY

This study numerically solves the inductionless MHD, momentum and energy equations. First given here are the continuity, momentum and energy equations in equations 2 to 4. Inductionless MHD equations for electric potential ϕ (Equation 5) and electric current density $\mathbf{j}$ (Equation 6) are then presented below, where the Lorentz force is the last term in Equation 3.The inductionless approximation is valid for flows with a low magnetic Reynolds number such as liquid metals at small length scales as in this study.

$$\frac{\partial \rho}{\partial t} + \nabla \cdot (\rho \mathbf{u}) = 0 \tag{2}$$

$$\rho \left(\frac{\partial \mathbf{u}}{\partial t} + (\mathbf{u} \cdot \nabla)\mathbf{u} \right) = -\nabla p + \nabla \cdot \left(\mu \left[\nabla \mathbf{u} + (\nabla \mathbf{u})^T - \frac{2}{3}(\nabla \cdot \mathbf{u})\mathbf{I} \right] \right) + \rho g + \frac{1}{\rho}(\mathbf{j} \times \mathbf{B}_0) \tag{3}$$

$$\rho \left(\frac{\partial h}{\partial t} + \nabla \cdot (h\mathbf{u}) \right) = \nabla \cdot (\kappa \nabla \theta) \tag{4}$$

$$\nabla^2 \phi = \nabla \cdot (\mathbf{u} \times \mathbf{B}_0) \tag{5}$$

$$\mathbf{j} = \sigma(-\nabla \phi + \mathbf{u} \times \mathbf{B}_0) \tag{6}$$

Open-source DNS code CHAPSim2 was used for this study (https://github.com/CCP-NTH/CHAPSim2). CHAPSim2 is a quasi-incompressible solver with variable thermal properties, developed for applications in the nuclear thermal-hydraulics community. A 2nd order central difference scheme is applied for spatial discretisation and a low-memory 3rd order Runge-Kutta scheme is applied for time advancement. Poisson equations for pressure and electric potential are solved using a 3D fast Fourier transform (FFT).

Geometry and Case Parameters

This study models a vertical channel with a height of 2δ, length of $10\pi\delta$ and width of $2\pi\delta$. One sided heating is imposed by a constant heat flux and the other wall is adiabatic. A Reynolds number of 10^4 and a heating of $Gr = 5 \times 10^7$ is used for all cases, where the characteristic length scale $L = 2\delta$. The working fluid is Lithium at an initial temperature of 570 Kelvin, with a Prandtl number of 0.04. Variable governing parameters for magnetic field strength (Ha) and stability parameter Π for different cases are presented in Table 1.

Inlet velocity is provided via an isothermal turbulence generator of $4\pi\delta$ length, at the same Reynolds number. A Neumann condition is specified for inlet temperature. Wall heating starts 2δ downstream from the inlet to allow for upstream conduction of temperature and to avoid a step change between the inlet flow and reversed heated flow.

Table 1. Governing parameters for different cases in the inclined magnetic field study

Case	$Ha_{\parallel}$	$Ha_{\perp}$	Gr	$\Pi_{\perp}$	$\Pi_{\parallel}$
A	0	0	5×10^7	0	0
B	100	0	5×10^7	25	0
C	0	100	5×10^7	0	25
D	100	100	5×10^7	25	25

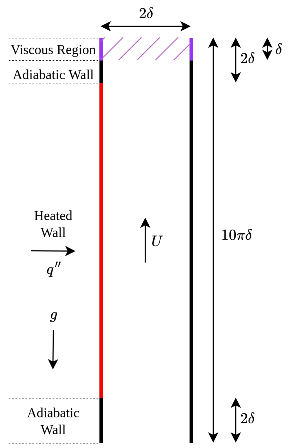

Figure 1. X-Y plane of domain configuration. Bulk velocity is denoted by U, gravity by g, constant heat flux q'' and dimensions are based on a half-channel height δ. The heated wall region is highlighted in red and the viscous outlet region is highlighted in purple.

The outlet boundary conditions need considerable attention due to strong numerical instabilities. Here, a Neumann outlet condition was applied for temperature and pressure and a convective boundary condition was applied for velocity, however strong convection with reversed flow across the boundary resulted in numerical instability. A domain length with a long unheated outlet is expected to overcome such instabilities but is not feasible in practice due to computational expense, therefore a 'viscous sponge' approach was implemented (Pant & Bhattacharya (2016)). Here an additional viscosity is smoothly applied to diffusivity terms in the momentum equations in directions normal to the flow in a short region before the outlet to damp out small-scale transverse velocity fluctuations. The viscosity in the streamwise direction is not altered, reducing the impact on the mean streamwise pressure gradient and the outlet region is excluded from analysis. The length of the viscous region is δ and viscosity is increased to a Reynolds number of 300. In addition, an adiabatic outlet length of 2δ is specified on the heated wall.

Resolution

Magneto-convection presents a numerically stiff problem. Spatial scales are very fine, with the formation of Hartmann layers on magnetic field-normal walls which approximately scale inversely with Hartmann number of the order of $\delta_{Ha} \approx \delta(Ha^{-1})$. Likewise, thermal dissipation requires a small timestep to ensure a Fourier number of less than 1.

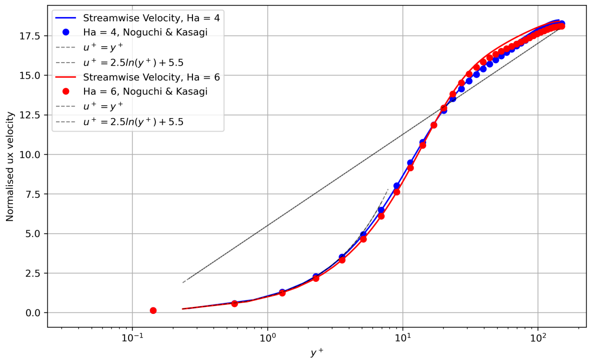

Figure 2. Streamwise velocity profiles (inner scale), normalised by u_τ.

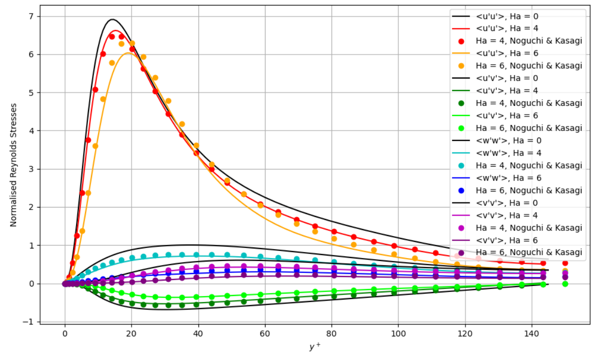

Figure 3. Components of Reynolds stresses, normalised by u_τ^2.

Large turbulent structures evolving over long timescales then require a very long period of averaging for statistical analysis. Here a timestep of 5×10^{-5} was used for all cases which ensured a Fourier number of ≈ 0.75. A mesh of 144 million grid points was used and a strong stretching was applied in the wall-normal direction to ensure a minimum of 10 mesh points within Hartmann boundary layers, as suggested by literature and confirmed by earlier study. Furthermore, the divergence of wall-normal current was tested for an isothermal simulation, which was resolved to machine accuracy. Key parameters are presented in Table 2. Further lengthscale analysis is required here to ensure results aren't restricted by the size of the domain.

Table 2. Mesh Resolution Parameters

Direction	L (δ)	No. of Cells	Δ^+
x	10π	1000	10.766
y	2	480	0.280 - 7.255
z	2π	300	7.178

VALIDATION

A canonical Hartmann channel flow with a transverse magnetic field was first studied to validate the solver against a DNS database (Ohtsubo *et al.* (1994)). Three cases of varying Hartmann number (0, 4, 6) and a bulk Reynolds number of 4610 were compared. Validation of CHAPSim2 against DNS reference data demonstrates good overall agreement in both velocity and Reynolds stresses. Suppression of turbulence, due to ohmic dissipation results in a lift of the log layer compared to a typical hydrodynamic flow, as can be seen in Figure 2. Figure 3 presents Reynolds stresses. CHAPSim2 gives a slightly lower magnitude of Reynolds stresses across statistics, especially with the higher Ha = 6 case. This could be attributed to the choice of flow forcing: reference data imposed a constant pressure gradient whereas a constant mass flux condition was applied here, allowing the shear velocity to vary. The shear Reynolds number was 3.5% lower than validation data for the Ha = 4 case and 5% lower for the Ha = 6 case. A slightly lower level of turbulence is therefore expected, in conjunction with the slightly higher streamwise velocity in the log layer exhibited in Figure 2.

RESULTS

Effects of a low Prandtl number fluid

First, results of reference case A are presented to isolate the phenomena associated with low Prandtl number heat transfer without a magnetic field. Velocity U_x, turbulent kinetic energy k and temperature θ profiles at different streamwise locations are presented in Figures 4 and 5. Rapid thermal diffusion quickly distributes the heat flux across the channel, providing an asymmetric buoyancy force across the channel. Flow is initially accelerated close to the heated wall, with a flattened profile at $x = 5$, before further developing into a strong turbulent jet. As the flow develops, the jet becomes more turbulent and deccelerates, coupled with a decrease in temperature gradient across the channel. Turbulent kinetic energy profiles in Figure 4 illustrate the progression of turbulence from the initially laminarised region near the wall at $x = 5$ to a much more uniform albeit assymetric profile at $x = 25$. Figure 6 illustrates general flow topography in a mid-slice of the domain in the x-y plane and a boundary layer slice at $y^+ \approx 15$.

Effects of different applied magnetic fields

Three different orientations of magnetic field were applied to the above reference case after it reached a statistically steady state: streamwise, wall-normal and a combination of the two, inclined at 45°. Given the orthogonal relationship between velocity and Lorentz force presented in Equations 5 to 6, only orientations where mean flow crosses magnetic field lines result in a strong flow opposing Lorentz force in a time-averaged sense. Therefore drastically different flow phenomena are observed between streamwise and wall-normal or inclined magnetic fields. The transient transformation of flow following application of the magnetic field was observed to be complex appearing to show two processes here: an initial rapid transformation of the existing turbulent structures and a regeneration of new flow structures, which takes place over a longer time. In a fusion reactor, we might expect to see both given a pulsed or steady regime in toroidal or poloidal ducts. Figure 7 illustrates the transformation of existing turbulent structures for a wall-normal magnetic field at 2.5, 7.5 and 17.5 seconds after the magnetic field is applied. An alignment of structures with magnetic field lines and destruction of turbulence, especially in the small scales is observed.

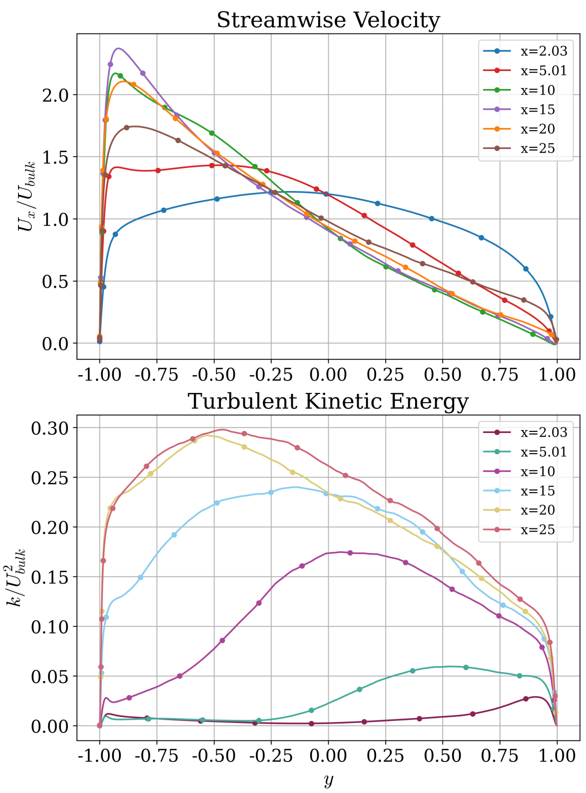

Figure 4. Time-averaged streamwise velocity and turbulent kinetic energy profiles at $x = 2$, $x = 5$, $x = 10$, $x = 15$, $x = 20$, $x = 25$. Values are normalised by U_{bulk} and U_{bulk}^2 respectively.

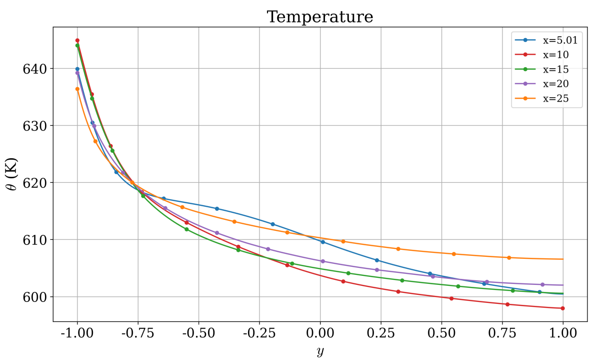

Figure 5. Time-averaged temperature profiles given in Kelvin at $x = 5$, $x = 10$, $x = 15$, $x = 20$ and $x = 25$.

Velocity, turbulent kinetic energy and temperature plots for streamwise and both wall-normal and inclined magnetic fields are presented in Figures 8, 9 and 10 respectively. Profiles and statistics are time-averaged over a period beginning after an initial strong change. Whilst not an accurate representation of a stationary turbulent flow due to residual slow transient variations, these provide some insight into flow properties over this change. Whilst all profiles are asymmetric, the flow-opposing Lorentz force in cases C and D significantly flattens velocity profiles, resulting in steep velocity gradients at the walls. In contrast, velocity profiles in case B elongate, with a stronger peak and accelerate as the flow develops with weak reversed flow observed on the opposite adiabatic wall. Interestingly, the stronger jet formed with a streamwise magnetic field increases turbulent kinetic energy compared to a flow without a magnetic field yet temperature gradients are also stronger,

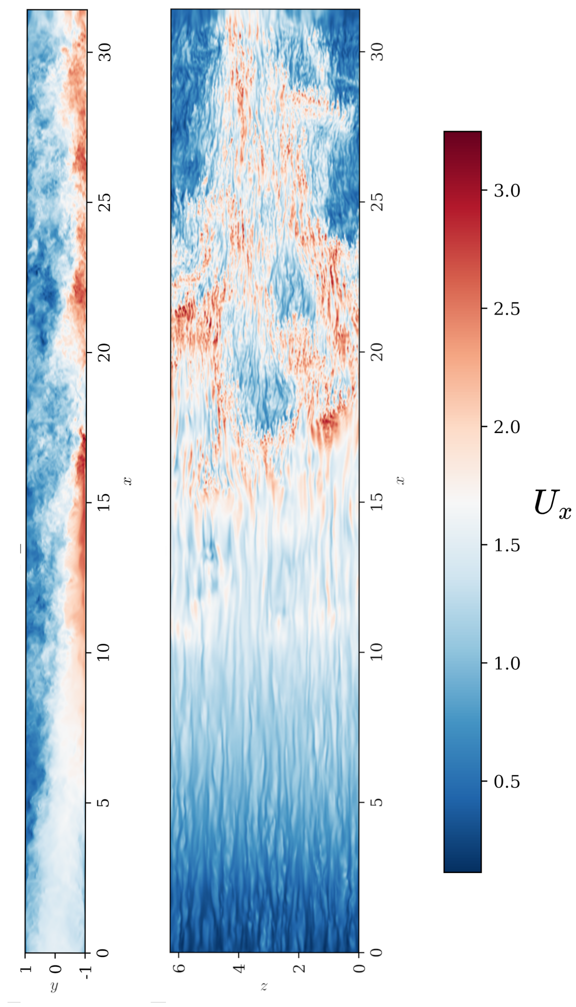

Figure 6. Instantaneous streamwise velocity of reference case A (no magnetic field applied) in the x-y and x-z planes at $z = \pi$ and $y^+ \approx 15$ respectively.

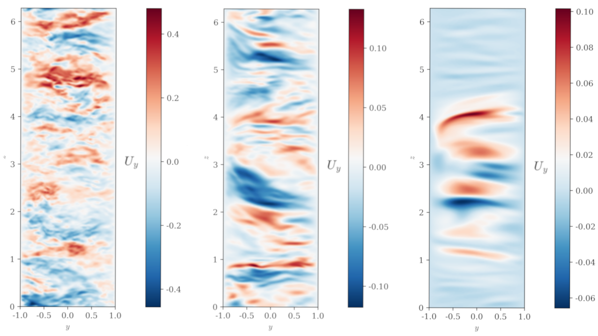

Figure 7. Instantaneous U_y in the $y - z$ plane at $x = 5\pi$ for case C, wall normal magnetic field. Snapshots are at t = 2.5, 7.5 and 17.5 seconds after a magnetic field is applied from left to right.

indicating decreased turbulent heat transfer. Instantaneous realisations of streamwise velocity for different magnetic fields are presented in Figure 11, at 7.5 seconds after magnetic fields were applied.

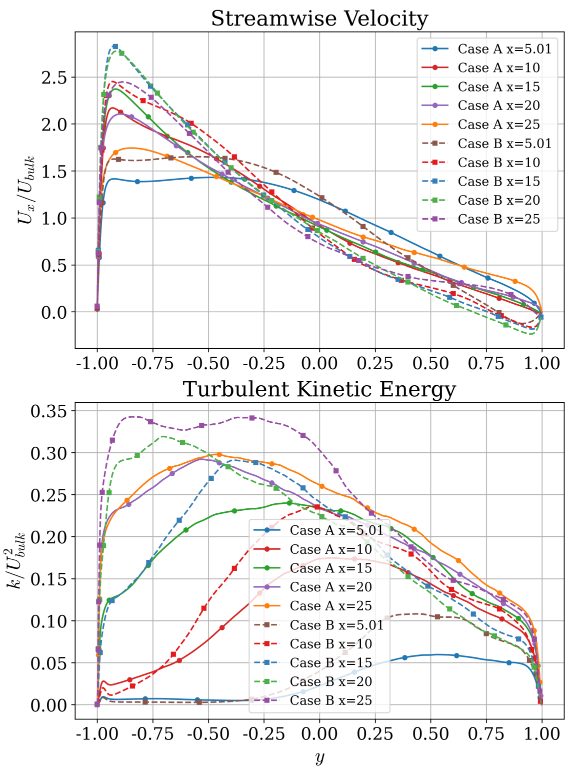

Figure 8. Time-averaged streamwise velocity profiles at $x = 5$, $x = 10$, $x = 15$, $x = 20$, $x = 25$ for cases A and B, reference case with no magnetic field and parallel magnetic field.

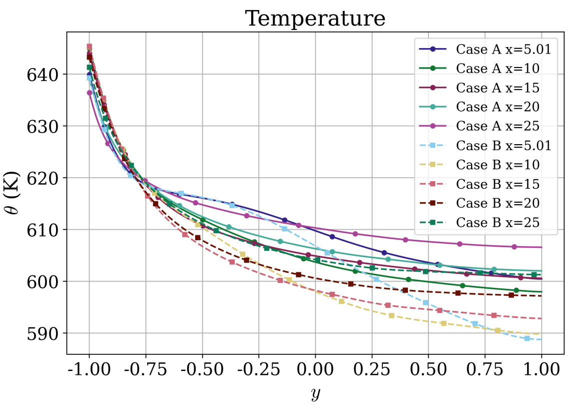

Figure 9. Time-averaged temperature profiles at $x = 5$, $x = 10$, $x = 15$, $x = 20$, $x = 25$ for cases A and B, reference case with no magnetic field and parallel magnetic field.

CONCLUSIONS

Whilst the results presented above are limited in scope, features of different magneto-convective flows are clearly apparent, in addition to low Prandtl number heat transfer phenomena. A clear distinction between the action of the Lorentz force on fluctuations, which here enhance buoyancy-driven jets and on the mean flow, which strongly suppresses turbulence can be seen, especially at the small scales leading to a dominance of larger scale structures. The combination of streamwise and wall-normal magnetic fields enhances turbulence suppression further, likely due to an additional component of joule dissipation but doesn't allow the growth of a jet due to the wall normal magnetic field component. The formation of magneto-convective fluctuations at this parameter range

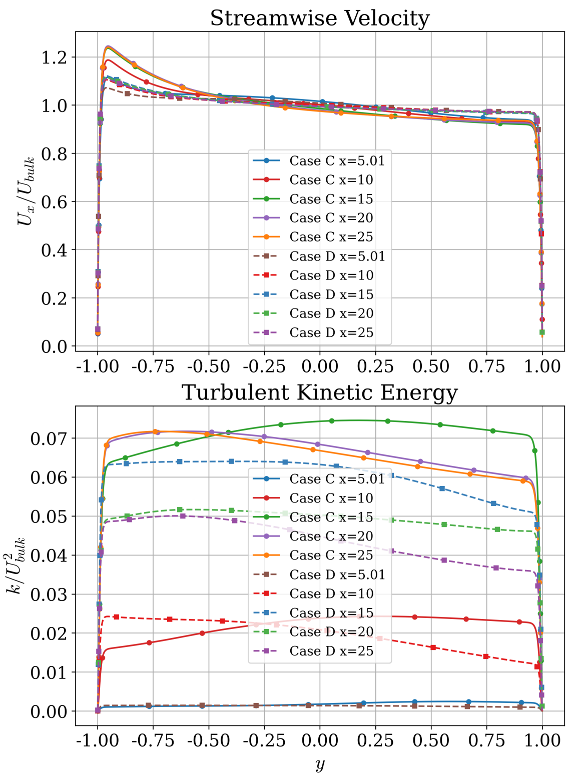

Figure 10. Time-averaged streamwise velocity and turbulent kinetic energy profiles at $x = 5$, $x = 10$, $x = 15$, $x = 20$, $x = 25$ for cases C and D, normal and inclined magnetic fields.

is unclear as a longer timescale is required to assess whether a stationary state of flow has been reached. Further in-depth statistical analysis over long timescales will be presented in future.

REFERENCES

A. Alemany, R. Moreau, P. L. Sulem & U. Frisch 1979 Influence of an external magnetic field on homogeneous MHD turbulence. *Journal de Mecanique* **18** (2), 277–312.

Lee, Donghoon & Choi, Haecheon 2001 Magnetohydrodynamic turbulent flow in a channel at low magnetic Reynolds number. *Journal of Fluid Mechanics* **439**, 367–394.

Ohtsubo, Y., Noguchi, H. & Kasagi, N. 1994 DNS database of turbulence and heat transfer.

Pant, Chandra Shekhar & Bhattacharya, Amitabh 2016 A viscous sponge layer formulation for robust large eddy simulation of thermal plumes **134-135**, 177–189.

Sommeria, JoëL & Moreau, René 1982 Why, how, and when, MHD turbulence becomes two-dimensional. *Journal of Fluid Mechanics* **118**, 507–518.

Vetcha, N., Smolentsev, S., Abdou, M. & Moreau, R. 2013 Study of instabilities and quasi-two-dimensional turbulence in volumetrically heated magnetohydrodynamic flows in a vertical rectangular duct **25** (2), 024102.

Zhang, Xuan & Zikanov, Oleg 2018 Convection instability in a downward flow in a vertical duct with strong transverse magnetic field. *Physics of Fluids* **30** (11), 117101.

Zikanov, Oleg, Belyaev, Ivan, Listratov, Yaroslav, Frick, Peter, Razuvanov, Nikita & Sviridov, Valentin 2021 Mixed Convection in Pipe and Duct Flows With Strong Magnetic Fields. *Applied Mechanics Reviews* **73** (1), 010801.

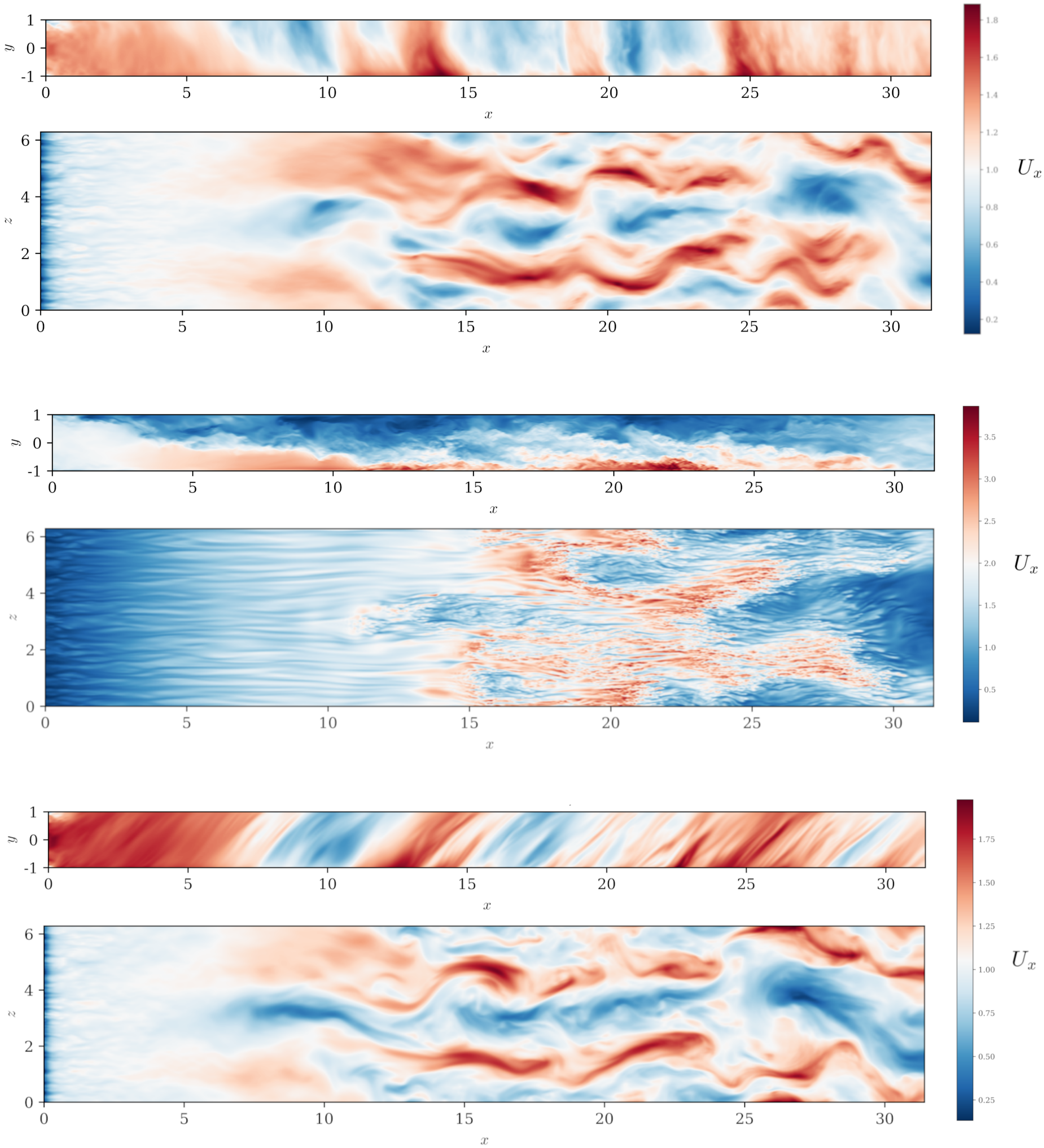

Figure 11. Instantaneous streamwise velocity of Cases C, B and D (top, middle and bottom), corresponding to wall-normal, streamwise and inclined magnetic fields. Slices are in the x-y and x-z planes at $z = \pi$ and $y^+ \approx 15$ respectively.